Sensitivity of tungsten neutron cross sections to target band mixing and β_6 deformation

J. P. Delaroche
Service de Physique Neutronique et Nucléaire, Centre d'Etudes de Bruyères-le-Chatel, 92542 Montrouge Cedex, France
(Received 9 July 1982)

It is shown that insertion of a deformation parameter β_6 in coupled channels calculations may be necessary for proper predictions of the neutron total cross sections (σ_T) at incident energies below $\sim$700 keV. This is illustrated in the present work with the σ_T measurements of Whalen *et al.* on the ^{182,184,186}W isotopes. In a previous report it has been established that these data could not be well reproduced using coupled channel calculations involving only β_2 and β_4 deformations. It is shown presently that this discrepancy can be removed if, provided that self-shielding corrections to these measurements are made, a small deformation parameter β_6 is considered in coupled channel analyses. As the W isotopes are lying at the rotational edge of the $A=190-200$ transitional mass region, it is also emphasized that band mixing effects on the model predictions might be of some importance. These effects have been investigated for ^{182,184,186}W as well as for ^{183}W using realistic collective wave functions.

[NUCLEAR REACTIONS Neutron total and scattering cross sections. Tungsten isotopes. Statistical model calculations. Realistic collective models. Coupled channels analyses. Deduced β_6 deformation parameters. Calculated inelastic cross sections for ground state and vibrational band levels.]

I. INTRODUCTION

In previous work by Delaroche *et al.*[1] the differential cross sections of measurements of neutron elastic and inelastic scattering from the ^{182,183,184,186}W isotopes at an incident energy of 3.4 MeV have been reported. These nuclei, lying at the rotational edge[2] of the $A=190-200$ transitional mass region, were assumed to be rigid rotors in the coupled channels (CC) analyses. With this assumption, especially rough for ^{183}W as is well known from Coulomb excitation measurements,[3] the analyses[1] which combine these scattering measurements and *s*- and *p*-wave strength functions[4] as well as total cross sections (σ_T) reported in a wide energy range[5-7] led to a satisfactory agreement between the calculations and most of the available neutron cross section measurements. However, as they seem related to the model assumptions made, a few problems are remaining. First of all, the model calculations failed to reproduce the experimental values[5] of σ_T at incident energies below $\sim$700 keV. In addition, it was found that the hexadecapole deformation parameter β_4 was significantly larger for ^{183}W than for ^{182}W and ^{184}W. As it was briefly discussed in Ref. 1, this result might depend on the rotational model (RM) assumption for this even-odd nucleus. On the other hand, recent measurements performed by Guenther and Smith[8] for the 2_γ^+ vibrational levels cannot be accounted for properly using the statistical model calculations described in Ref. 1. Thus, it is necessary to consider calculations of the direct interaction cross section for these excited states, on the basis of realistic collective wave functions.

The present work is an extension of the reported study on neutron scattering from the tungsten isotopes.[1] Its aim is (i) to investigate the band mixing and β_6 deformation effects on fast neutron scattering from these nuclei in order to understand the origin of the problem mentioned above and (ii) to estimate the magnitude of the direct interaction cross sections for vibrational states at low excitation energy. Coupled channels calculations are presented, which involve Kumar's[9] and Faessler *et al*'s.[10] wave functions available for the even-even W isotopes, and Kerman's[11] and Casten *et al.*'s[12] wave functions adjusted on the strongly mixed rotational bands of ^{183}W.

II. COUPLED CHANNELS CALCULATIONS

In the following CC calculations the optical potential U and deformation parameters β_2 and β_4 are

identical to those given in Ref. 1. The potential U may be expressed as:

$$U=-(V+iW_v)f(r,a_v,R_v)$$
$$+4ia_D W_D \frac{d}{dr}f(r,a_D,R_D)$$
$$+2\lambda\!\!\!^{-}_{\pi}{}^2 V_{so}\,\vec{l}\cdot\vec{s}\,\frac{1}{r}\frac{d}{dr}f(r,a_{so},R_{so}) ,$$

where $f(r,a_i,R_i)$ is a Woods-Saxon form factor. As in Ref. 1, the potential U is expanded into spherical harmonics Y^0_λ (with $\lambda \leq 8$). In the present work we are dealing with an energy range $E \lesssim 4$ MeV where the volume absorptive potential W_v has been neglected. For the sake of completeness, parameters of the potential are given in Table I. No further optimization of these parameters has been attempted since the purpose of the present work is to estimate band mixing and β_6 deformation effects. Only a minor adjustment of W_D had to be made, as is explained in Sec. IV. The coupled channels analyses have been performed using the code ECIS 78 (Ref. 13) in a manner similar to that described by Baker *et al.*[14] in their analyses of (α,α') scattering measurements from osmium isotopes. Although approximate, this method has proved successful in the analyses of (α,α'),[14,15] (^{12}C, ^{12}C′),[16] (p,p'),[17] and (n,n')[18] scattering from some transitional nuclei. Briefly, the potential form factors U_λ were calculated[14] in the rotational model framework and the band mixed wave functions $|IM\rangle$ of the target nucleus were inserted into ECIS 78 as computational inputs through the corresponding reduced matrix elements $\langle J||M(E\lambda)||I\rangle$ of the collective electric multipole operators $M(E\lambda)$.[19]

In the present work, the notation

$$M^{(\lambda)}_{IJ}=i^\lambda\langle J||M(E\lambda)||I\rangle \tag{1}$$

used currently by spectroscopists for the reduced matrix elements (RME) has been adopted.[20] The RME values satisfy the following symmetry relation:

$$M^{(\lambda)}_{JI}=(-)^{\lambda+J-I}M^{(\lambda)}_{IJ} , \tag{2}$$

and are related to the reduced $E\lambda$ transition probabilities $B(E\lambda)$ and spectroscopic quadrupole moments Q_I. These relationships[21] are, respectively,

$$B(E\lambda;I\rightarrow J)=\frac{1}{(2I+1)}\,|M^{(\lambda)}_{JI}|^2 \tag{3}$$

and

$$Q_I=\left[\frac{16\pi}{5}\right]^{1/2}\left[\frac{I(2I-1)}{(I+1)(2I+1)(2I+3)}\right]^{1/2}$$
$$\times M^{(2)}_{II} . \tag{4}$$

In principle, any collective model would be able to provide all the $M^{(\lambda)}_{IJ}$ values for $\lambda \geq 2$. This would be the case for the dynamic deformation theory[2,9] (DDT), and the rotation vibration model[10] (RVM) which both describe quite well the low energy collective properties of ^{182,184,186}W. The level schemes[22] for these nuclei are shown in Fig. 1 and, for ^{186}W, the comparison between experimental and RVM predicted level schemes is presented in Fig. 2. The rotation particle coupling (RPC) model[11,23,24] would also be able to provide RME values for ^{183}W. Unfortunately, the only available RME's from (i) DDT and RPC, and (ii) RVM models are $M^{(2)}_{IJ}$ (Refs. 9 and 23) and $M^{(\lambda)}_{IJ}$ for $\lambda=2,4$ (Ref. 10), respectively. Part of the present work has been done in order to compare the CC calculations (see the next sections) based on DDT, RVM, RPC, and RM (Ref. 25) models. For this purpose, the multipole operators $M(E6)$ and $M(E8)$ and their respective RME values have been determined from RVM (see Appendix A), and the RME values from DDT and RPC models have been estimated for the operators $M(E4)$, $M(E6)$, and $M(E8)$ (see Sec. IV A). Finally, it must be pointed out that the $M^{(2)}_{IJ}$ values from the RPC model have been calculated using Kerman's[11] and Casten *et al.*'s[12] admixed amplitudes (see Appendix B). The reduced matrix elements involved in the present work are given in Tables II–IV.

TABLE I. Tungsten isotopes. Neutron optical potential and deformation parameters determined in a previous work (see Ref. 1). Strengths in MeV; geometry parameters in femtometers. Incident neutron energy E in MeV; $E < 9$ MeV.

$V=49.90-16.00\left[\frac{N-Z}{A}\right]-0.25E$	$W_D=4.93-8.00\left[\frac{N-Z}{A}\right]+1.30E^{1/2}$	$V_{so}=6.00$
$r_V=1.26$	$r_D=1.28$	$r_{so}=1.26$
$a_V=0.63$	$a_D=0.47$	$a_{so}=0.63$
^{182}W: $\beta_2=0.223\pm0.007$, $\beta_4=-0.054\pm0.006$.	^{183}W: $\beta_2=0.220\pm0.012$, $\beta_4=-0.075\pm0.010$	
^{184}W: $\beta_2=0.209\pm0.009$, $\beta_4=-0.056\pm0.006$.	^{186}W: $\beta_2=0.203\pm0.006$, $\beta_4=-0.057\pm0.006$	

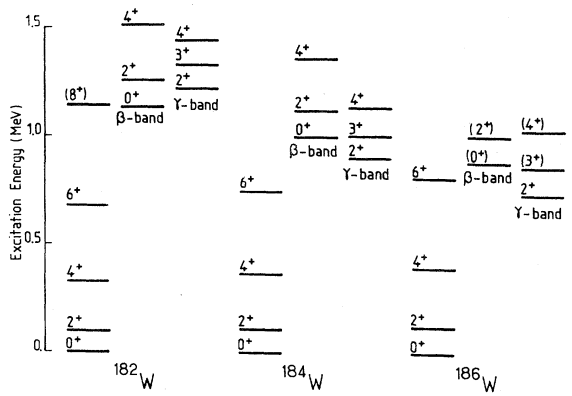

FIG. 1. Level schemes of even tungsten isotopes at low excitation energies (Ref. 22). Ground state band ($K=0$), β-vibrational band ($K=0$), and γ-vibrational band ($K=2$).

III. HEXACONTATETRAPOLE (β_6) DEFORMATION EFFECTS

As pointed out in Ref. 1 the CC calculations based on the simple rotational model are able to reproduce with a good accuracy (i.e., better than 5%) the energy variations of the ^{182,184,186}W total cross sections measured[6,31] at incident energies (E) higher than $\sim$700 keV, but fail below this energy if one considers Whalen *et al.*'s[5] σ_T measurements. The self-shielding corrections[32] made recently[31] to these measurements are appropriate to restore fair fits for σ_T (^{184}W) and σ_T (^{186}W). Although they also produce a substantial effect on the measured[5] σ_T (^{182}W) values, the self-shielding corrections are not large enough to remove all the deviations between the calculations[1] and the corrected σ_T values[31] for ^{182}W. The "residual" discrepancy should reflect the effect of a specific property of this even-A W isotope.

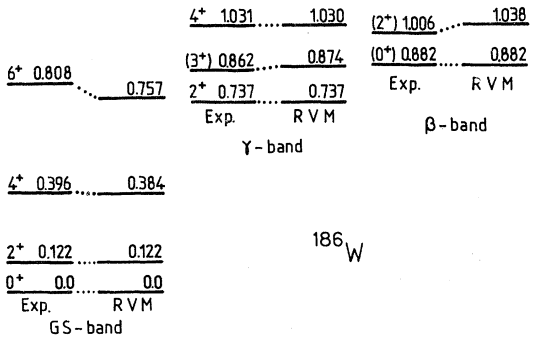

FIG. 2. Ground state, β- and γ-vibrational bands for ^{186}W. The experimental energy, spin, and parity values are from Ref. 22 and compared with the rotation vibration model predictions (Ref. 10). Energies are in MeV.

Thus, in order to improve the fit, a deformation parameter β_6 has been included in new CC calculations. This is achieved by expressing the potential radius R_i as follows:

$$R_i = r_i A^{1/3}\left[1+\sum_{\lambda'=2,4,6}\beta_{\lambda'}Y^0_{\lambda'}\right] .$$

Several attempts have been made previously in order to determine β_6 from hadron scattering for some W isotopes. Analyzing an (α,α') inelastic scattering measurement for ^{182}W at 60 MeV, Hendrie *et al.*[33] found that a small, if any, β_6 deformation parameter would be needed to reproduce the data. Recently a (p,p') inelastic scattering measurement has been performed at 35 MeV incident energy[34] for ^{186}W; unfortunately, a complete analysis of these data is not yet available. On the other hand, it is expected from Nilsson *et al.*'s structure calculations[35] that β_6 is small and negative ($\beta_6\sim-0.01$) for ^{182}W and negligible for ^{186}W. These values have been presently considered as indicative since the experimental values of β_6 reported in the rare earth region deviate strongly from the model predictions (see Fig. 11 of Ref. 35). A few CC calculations have been performed in the present work assuming $\beta_6\neq0$. Some results shown in Fig. 3 support a small negative β_6 value for ^{182}W. Similar results have been obtained for ^{184}W and ^{186}W. It seems that the following values,

$$\beta_6(^{182}\mathrm{W})\sim-0.04 ,$$

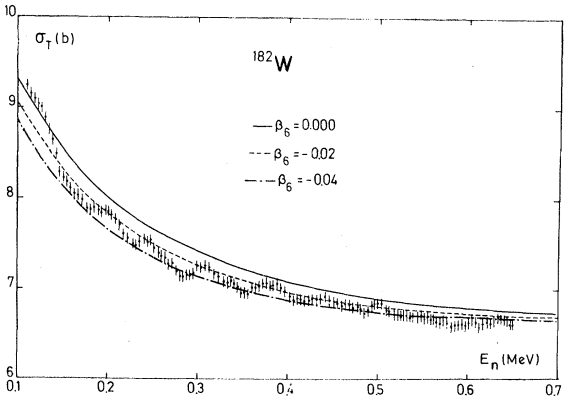

FIG. 3. Energy variation of the total cross section σ_T (^{182}W) at incident energies below $\sim$700 keV. The experimental data are taken from Ref. 31. The full, dashed, and dotted-dashed curves represent coupled channels calculations performed assuming $\beta_6=0.$, -0.02, and -0.04, respectively (see Sec. III).

and

$$|\beta_6(^{186}\mathrm{W})| < |\beta_6(^{184}\mathrm{W})| < |\beta_6(^{182}\mathrm{W})| ,$$

would be appropriate for fitting quite well the corrected σ_T values[31] for the three isotopes. The effect of this β_6 parameter on the calculated σ_T (^{182}W) is $\sim 4\%$ at $E \sim 100$ keV and decreases with energy, as can be seen in Fig. 3. Of course the uncertainties attached to the β_6 values are probably large (typically $\sim 50\%$) since the values given above are correlated with the values of β_2 and β_4 determined previously[1] (Table I). An additional support of a small negative β_6 value is provided by the inelastic scattering cross sections for the first 2^+ and 4^+ excited states[1]. Figure 4 shows a better agreement between experimental and presently calculated angular distributions for ^{182}W at 3.4 MeV incident energy if a β_6 value of -0.04 is included in the CC calculations. Similar improvements are found for ^{184,186}W. Furthermore, the inclusion of β_6 in the CC calculations does not change the calculated total cross sections by more than $\sim 1\%$ at 3.4 MeV, and, more generally, at energies above 1 MeV. All these considerations corroborate a specific β_6 effect on the neutron scattering properties of ^{182,184,186}W.

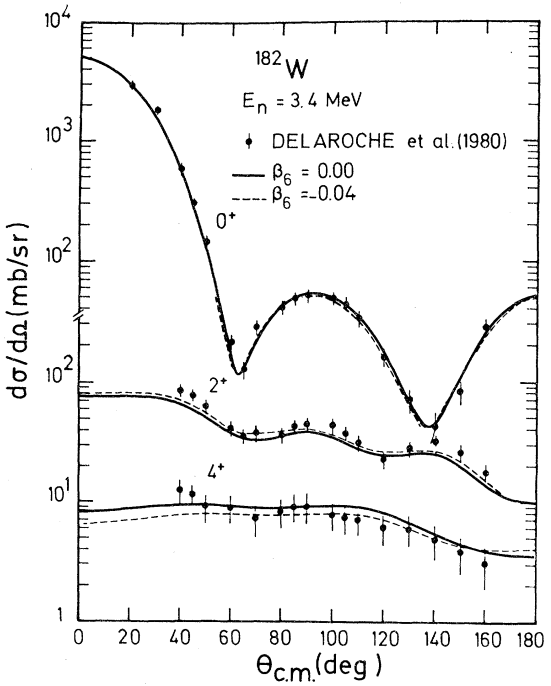

FIG. 4. Elastic and inelastic scattering angular distributions for ^{182}W at 3.4 MeV incident energy. The experimental data and calculations based on symmetric rotational model assumptions (full lines) are taken from Ref. 1; the dashed lines result from similar calculations for $\beta_6 = -0.04$.

An investigation of the target band mixed wave function effect on the calculated σ_T must be performed since band mixing phenomena might also alter the calculated values of the cross sections. These structure properties of the even W isotopes extensively studied by Kumar and Baranger[2] are considered in the following section.

IV. BAND MIXING EFFECTS

Band mixing effects are investigated in Sec. IV A for the even W isotopes, and in Sec. IV B for ^{183}W.

A. Even W isotopes

Let us search for a possible departure from the rotational model predictions, discussed in Ref. 1 for both total cross sections and inelastic scattering cross sections for the 2^+ and 4^+ states belonging to the ground state (g.s.) "band," when target band mixed wave functions $|IM\rangle$ are used in the CC calculations. These wave functions may be written as:

$$|IM\rangle = \sum_K A_K^I |IMK\rangle ,$$

where A_K^I is a mixing amplitude, and $|IMK\rangle$ the eigenfunction of the symmetric top Hamiltonian. From these wave functions we can also estimate the direct interaction (DI) cross sections for the β- and γ-vibrational states. The present study has been restricted to the 0_β^+ (^{182}W) and 2_γ^+ (^{184,186}W) levels for which a few inelastic scattering measurements are available.[8,31,36,37] In the following discussion we will mainly consider the nucleus ^{186}W.

As explained in Sec. II the band mixed wave functions $|IM\rangle$ have been inserted into ECIS 78 through the corresponding reduced matrix elements defined in Eqs. (1)–(4). We have considered here the RME values obtained from DDT and RVM. The $E2$ DDT reduced matrix elements have been taken from Ref. 9. In calculations involving these $E2$ RME's, the $E\lambda$ reduced matrix elements for $\lambda > 2$ have been assumed to be those of a simple rotor[25] since, unfortunately, they have not been reported by Kumar in Ref. 9. Just the opposite, the RVM reduced matrix elements have been calculated using equations and tabulations given in Ref. 10. Analytic expressions for the $E6$ and $E8$ reduced matrix elements have been determined in the present work. These expressions as well as those for

$E2$ and $E4$ transitions are given in Appendix A in a suitable form for the present calculations.

For $E2$ transitions, these are compared in Table III with the values inferred by the measurements of $B(E2)$ available[26–30] for ^{186}W. From Tables II and III it can be seen that both DDT and RVM predict $E2$ RME values in agreement with measurements. The DDT and RVM predictions for $M_{IJ}^{(2)}$ relative to the 0^+, 2^+, 4^+ levels of the g.s. band deviate by less than $\sim 9\%$. For other kinds of transitions from the g.s. band levels to the 2_γ^+ or 0_β^+ excited state, the deviation between the $E2$ RVM and DDT reduced matrix element values seem to be more important. Presently, the DDT and RVM predictions cannot be verified for transitions leading to the 0_β^+ and 2_γ^+ excited states since the Coulomb excitation measurements now available are very scarce. However, neutron inelastic scattering might bring some substantial information.

1. *Ground state band levels*

Using DDT and RVM reduced matrix elements and assuming the coupling basis $(0^+,2^+,4^+)$ and the potential parameters given in Table I, CC calculations have been performed for σ_T and inelastic scattering to the first 2^+ and 4^+ excited state at 3.4 MeV incident energy. Below ~ 700 keV, DDT and RVM lead to calculated σ_T values which deviate from the CC calculations of Ref. 1 by less than 0.6% for ^{186}W as well as for ^{184,186}W. Thus it is clear that band-mixing effects on σ_T at low energies are very small and do not contribute significantly to the solution of the σ_T discrepancy considered in Sec. III. The calculations based on the DDT wave functions performed at 3.4 MeV for elastic and inelastic scattering from ^{186}W are shown as dashed lines in Fig. 5; the curves include compound nucleus (CN) and direct interaction (DI) contributions. The calculations based on the RVM wave functions, not shown in Fig. 5, give results very similar to those based on the DDT wave functions. It can be seen that, at this energy, the band mixing effects are small. The fact that the full (RM) and dashed (DDT) curves are almost identical is not surprising since all these models produce similar $E2$ RME values (see Tables II and III) for the g.s. band tran-

TABLE II. Relative $E2$ reduced matrix element values (in barns) used in the coupled channels calculations for ^{182,184,186}W.

I^c	J^c	^{182}W	^{184}W	^{186}W
0^+	2^+	−1.000	−1.000	−1.000
0^+	2_γ^+	−0.085[a]	−0.149[a]	−0.209[a]
2^+	2^+	1.185[a]	1.155[a]	1.096[a]
		1.195[b]	1.195[b]	1.195[b]
2^+	2_γ^+	−0.360[a]	−0.484[a]	−0.658[a]
2^+	4^+	−1.645[a]	−1.660[a]	−1.679[a]
		−1.603[b]	−1.603[b]	−1.603[b]
2_γ^+	2_γ^+	−0.090[a]	−0.500[a]	−0.738[a]
2_γ^+	4^+	0.230[a]	0.206[a]	0.171[a]
4^+	4^+	1.530[a]	1.500[a]	1.444[a]
		1.529[b]	1.529[b]	1.529[b]
0_β^+	2^+	−0.205[a]	−0.247[a]	−0.273[a]
0_β^+	2_β^+	−0.460[a]	−0.680[a]	−0.946[a]
0_β^+	2_γ^+	0.865[a]	0.814[a]	0.727[a]
2_β^+	2_β^+	0.205[a]	0.747[a]	1.214[a]
0^+	2_β^+	−0.210[a]	−0.191[a]	−0.155[a]
2^+	2_β^+	−0.145[a]	−0.098[a]	−0.053[a]
4^+	2_β^+	−0.290[a]	−0.397[a]	−0.513[a]
2_γ^+	2_β^+	−1.110[a]	−0.990[a]	−0.754[a]

[a]DDT value (see Ref. 9).
[b]RM value (see Ref. 25).
[c]Following O'Brien *et al.* (Ref. 26) the first 2^+ state predicted (Refs. 2 and 9) beyond the first excited state has been identified to the 2_γ^+ state; the second one (Refs. 2 and 9) has then been identified to the 2_β^+ state.

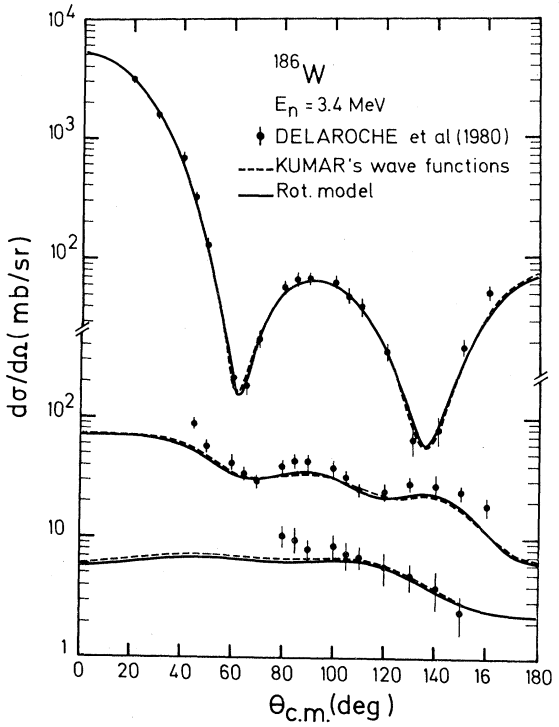

FIG. 5. Elastic and inelastic scattering angular distributions for ^{186}W at 3.4 MeV incident energy. The experimental data and calculations (full lines) are taken from Ref. 1. The dashed curves result from similar calculations in which Kumar's $E2$ reduced matrix elements of Ref. 9 are used (see Sec. IV).

TABLE III. Relative $E2$, $E4$, $E6$, and $E8$ reduced matrix element values for ^{186}W. Comparison between rotation vibration model (RVM), rotational model (RM), and measurements (exp).

I	J	$E2$ (b)			$E4$ (b^2)		$E6$ (b^3)		$E8$ (b^4)	
		RVM[a]	RM[e]	exp[g]	RVM[a]	RM[e]	RVM[a]	RM[e]	RVM[a]	RM[e]
0^+	2^+	−1.000	−1.000		0.000	0.000	0.000	0.000	0.000	0.000
0^+	2^+_γ	−0.237	0.000	0.207±0.007[b,c]	0.000	0.000	0.000	0.000	0.000	0.000
2^+	2^+	1.195	1.195	1.172±0.052[b,h]	1.160	1.195	0.000	0.000	0.000	0.000
2^+	2^+_γ	−0.445	0.000	0.314±0.012[b,c]	0.257	0.000	0.000	0.000	0.000	0.000
2^+	4^+	−1.664	−1.603	1.526±0.064[b,c]	−1.104	−1.140	−1.356	−1.254	0.000	0.000
2^+_γ	2^+_γ	−1.135	0.000	−0.917±0.221[d]	0.431	0.000	0.000	0.000	0.000	0.000
2^+_γ	4^+	−0.095	0.000		0.792	0.000	−0.305	0.000	0.000	0.000
4^+	4^+	1.457	1.529	~1.529[f]	1.132	1.207	1.195	1.122	1.384	1.347
0^+	4^+	0.000	0.000		1.000	1.000	0.000	0.000	0.000	0.000

[a]See Ref. 10.
[b]Absolute value.
[c]See Ref. 27.
[d]See Ref. 26.
[e]See Ref. 25.
[f]See Ref. 28.
[g]In e b units.
[h]Rotational model value obtained from the combination of the $B(E2;0^+\rightarrow 2^+)$ value (Ref. 29) for ^{182}W (nucleus which may be assumed a "good" rotor) with the measured ratio (Ref. 30) of the ^{182,186}W quadrupole moments Q_{2+}.

sitions as emphasized above. Similar results are obtained for the ^{182,184}W scattering cross sections, and, in addition, the total cross sections predicted by the three models are almost identical. Thus it is well justified to have assumed in Ref. 1 rotational model wave functions for the 2^+ and 4^+ g.s. levels, and to consider that band mixing effects are not as important as the β_6 deformation effect discussed in Sec. III.

2. β- and γ-vibrational states

Let us now consider the DDT and RVM wave functions in view of predicting the DI cross sections for the β- and γ-vibrational bandhead levels.[22] For this purpose, the coupling bases $(0^+,2^+,4^+,0^+_\beta)$ and $(0^+,2^+,4^+,2^+_\gamma)$ have been considered. As pointed out in Sec. II, the surface absorptive potential W_D of Ref. 1 has been slightly decreased by 8% because the coupling basis is presently larger. The calculation results are shown in Figs. 6–8. As can be seen on Fig. 6, the fit to the cross section measured[36] at 2.7 MeV for the 0^+_β (^{182}W) bandhead level is improved when the DI contribution is taken into account though the data are somewhat scattered. Unfortunately, at this incident energy, the strong CN contribution does not permit us to accurately evaluate the DI contribution.

Experimental and calculated cross sections for the 2^+_γ states of ^{184,186}W are shown in Figs. 7 and 8, respectively. It can be seen in Fig. 7, which displays the inelastic scattering excitation function[8,36,37] for the 2^+_γ (^{184}W) level at energies between threshold and 4 MeV, that the CN cross section determined from Ref. 1 lies below the experimental

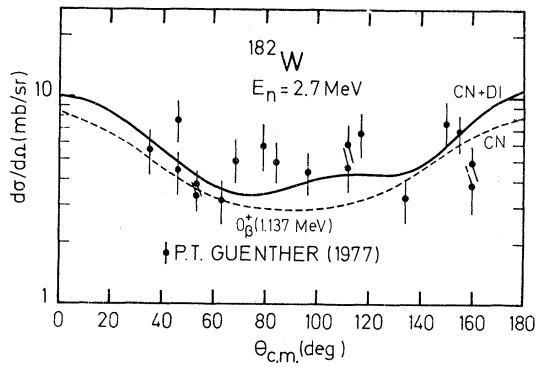

FIG. 6. Inelastic scattering angular distribution to the 0^+_β ($K=0$ bandhead) state of ^{182}W at 2.7 MeV incident energy. The data are from Ref. 36. The dashed curve (CN) represents the compound nucleus cross section. The full line is the sum of CN and DI components calculated using Kumar's $E2$ reduced matrix elements (Ref. 9).

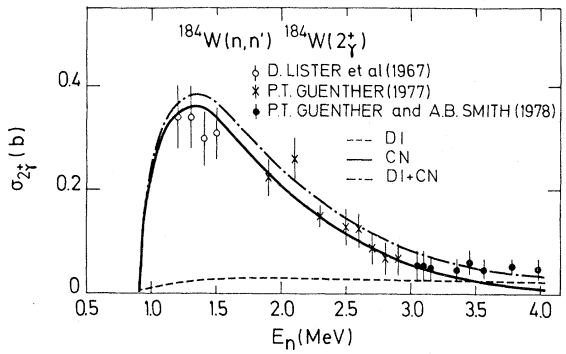

FIG. 7. Inelastic scattering excitation function for the 2_γ^+ ($K=2$ bandhead) state of ^{184}W. The full line (CN) represents the statistical model component calculated from Ref. 1. The dashed line (DI) is for the direct scattering (see Sec. IV) from this state as calculated from Kumar's $E2$ reduced matrix elements (Ref. 9). The dotted-dashed curve represents the sum of CN and DI components. The data are from Refs. 8, 36, and 37.

data at $E \gtrsim 3.4$ MeV. Attempts have been made to increase the CN cross section in this energy region performing new statistical model (SM) calculations for which the target level density parameters have been varied within their respective estimated uncertainties. As we have excluded the possibility of making a local SM fit, we found that the CN cross section might not be increased by more than $\sim 10\%$. This value may be considered as an upper limit since the SM calculations should have been

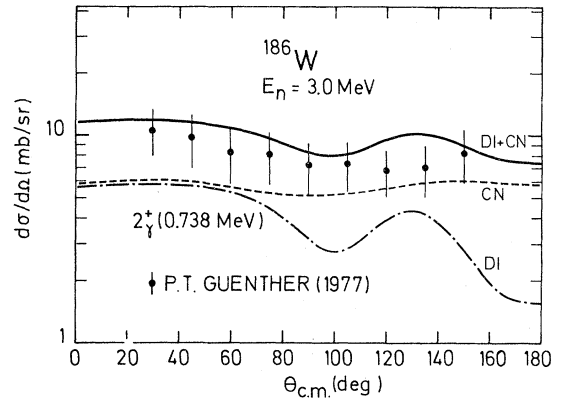

FIG. 8. Inelastic scattering angular distribution to the 2_γ^+ ($K=2$ bandhead) state of ^{186}W at 3 MeV incident energy. The data are from Ref. 36. The dashed line (CN) represents the compound nucleus cross section. The direct interaction (DI) calculated assuming Kumar's $E2$ reduced matrix elements (Ref. 9) is represented by the dotted-dashed line. The full line is the sum of CN and DI cross sections.

performed using neutron transmission coefficients obtained from CC calculations made with a coupling basis $(0^+,2^+,4^+,2_\gamma^+)$ and an absorptive potential W_D smaller than that given in Ref. 1.

From this discussion, it seems necessary to add a DI component to the CN cross section in order to obtain a good fit at $E \gtrsim 3.4$ MeV. CC calculations based on the DDT wave functions[9] produce a DI cross section (dashed line) with the correct order of magnitude (Fig. 7). At energies below 3 MeV, the sum of CN and DI cross sections, represented as a dotted-dashed line, lies slightly above the measurements.[36,37] This result must not be considered puzzling, at present, since the SM predictions (full line) are probably too large in that energy range (see the discussion above).

A direct interaction mechanism for scattering from the 2_γ^+ (^{186}W) level has also been considered. This is illustrated in Fig. 8 which shows experimental and calculated differential cross sections at 3 MeV. The measured angular distribution[36] displays a structure which departs slightly from the symmetry with respect to $\theta_{\text{c.m.}}=90°$ which is the signature[38] of the CN mechanism; moreover, the measurements lie above the CN cross section (dashed line) determined from Ref. 1. Further statistical model calculations are not significantly able to improve the fit to the data (see the discussion above). After adding to the CN cross section the DI cross section calculated using DDT wave functions,[9] a better agreement is found between measurements and predictions (full line).

It can be concluded from the analyses above that to within a minor adjustment of the absorptive potential depth W_D of Table I, it is possible to determine in a straightforward manner, from microscopic grounds,[2,9] the correct order of magnitude of the DI cross sections for the 0_β^+ (^{182}W) and 2_γ^+ (^{184,186}W) levels, which are nevertheless small.

Unfortunately, these calculations based on the $E2$ reduced matrix elements from DDT are not fully satisfactory because the $E\lambda$ reduced matrix elements have not been considered for $\lambda > 2$. Therefore, more complete CC calculations have been performed using RME determined for $\lambda \geq 2$ in the framework of the rotation vibration model[10] (see Appendix A). Theoretical cross sections predicted at 3 MeV for the 2_γ^+ (^{186}W) excited state are shown in Fig. 9. The coupling basis $(0^+,2^+,4^+,2_\gamma^+)$ and the potential parameters of Table I have been used in the CC calculations. The dotted-dashed line represents the result of a calculation in which only the $E2$ RME's for transitions between the g.s. levels

and the 2^+_γ state have been considered; the full (dotted) line is obtained from the calculations in which the $E4$ ($E4$ and $E6$) RME's have been considered in addition to the $E2$ reduced matrix elements.

From Fig. 9 it can be seen that $\sigma(2^+_\gamma)$ depends mainly on the $E2$ and $E4$ RME values and that the effect of the $E4$ reduced matrix elements is to increase by $\sim 20\%$ the $\sigma(2^+_\gamma)$ value calculated assuming only $E2$ reduced matrix elements. The inclusion of a small β_6 value in the calculations does not alter this enhancement. Also shown on Fig. 9, as a dashed line, is the 2^+_γ cross section determined using $E2$ reduced matrix elements from DDT. Since this curve closely follows the dotted-dashed line, one may speculate that the dynamic deformation theory and the rotation vibration model would lead to approximately similar predictions for $\sigma(2^+_\gamma)$ from calculations involving all $E\lambda$ RME's.

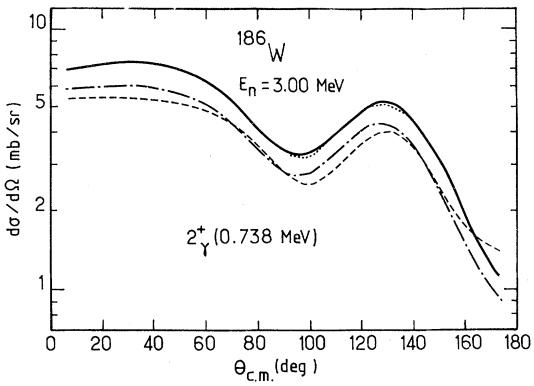

FIG. 9. Direct interaction cross section for the 2^+_γ ($K=2$ bandhead) state of ^{186}W, at 3 MeV incident energy. The curves result from $(0^+,2^+,4^+,2^+_\gamma)$ coupled channels calculations based on (a) Kumar's $E2$ reduced matrix elements (Ref. 9) (dashed line), and (b) Faessler *et al.*'s (Ref. 10) wave functions when: $E2$ (dotted-dashed line); $E2$ and $E4$ (full line); $E2$, $E4$, and $E6$ (dotted line) reduced matrix elements for the transitions leading to the 2^+_γ state are inserted, respectively, in the CC calculations (see Sec. IV).

B. ^{183}W

The low-lying level properties of the ^{183}W nucleus have been extensively studied by Kerman,[11] Rowe,[24] Brockmeier *et al.*,[23] and, more recently, by McGowan *et al.*[3] From these investigations it appears that the rotation particle coupling (RPC) model provides a clear understanding of the electromagnetic properties of the ^{183}W low-lying excited states. Considering that the effect of core vibration is negligible, this nucleus exhibits two rotational bands built on the close $K^\pi=\frac{1}{2}^-$ and $K^\pi=\frac{3}{2}^-$ intrinsic states. Following Brockmeier *et al.*[23] it is presently assumed that ^{183}W has an axially symmetric deformation.

Using the notations of Ref. 39, the ^{183}W wave functions can be written as

$$|IM\rangle=\sum_{K,\nu}\alpha^I_{K,\nu}\,|IMK,\nu\rangle\ ,$$

with

$$|IMK,\nu\rangle=\left[\frac{2I+1}{16\pi^2}\right]^{1/2}\{D^{I*}_{MK}(\Omega')\,|\phi_{K,\nu}\rangle+(-)^{I+K}D^{I*}_{M-K}(\Omega')\,|\bar{\phi}_{K,\nu}\rangle\}\ ,$$

where $|\phi_{K,\nu}\rangle$ and $|\bar{\phi}_{K,\nu}\rangle$ represent intrinsic states, D^I_{MK} are rotation functions, and ν is an index running over different intrinsic states having the same K quantum number. Although these states $|IM\rangle$ can be inserted in the coupled channels formalism, provided that the optical potential is modified accordingly,[39] we have decided to perform the CC calculations for ^{183}W in a manner similar to that explained in Sec. II. The reduced matrix elements $\langle I||M(E2)||J\rangle$ of the quadrupole operator $M(E2)$ have been determined from the method explained in Appendix B. Some numerical values of these RME's, gathered in Table IV, have been calculated assuming Kerman's[11] or Casten *et al.*'s[12] mixing amplitudes and used in CC calculations at 3.4 MeV with the g.s. band states from $\frac{1}{2}^-$ to $\frac{9}{2}^-$ as the coupling basis.[1] They are given in Fig. 10 where the dashed and dotted-dashed lines represent the sums of DI and CN components; also shown in this figure are the measurements and calculations (full lines) based on the simple rotational model.[1] Since predictions are very similar, it seems not necessary to significantly change the β_2 and β_4 values for ^{183}W (see Table I) which, in addition, are in excellent agreement with Casten *et al.*'s[40] ϵ_2 and ϵ_4 deformations, when converted into β_2 and β_4.

V. CONCLUSION

It has been shown in the present work, on the study of neutron interactions with tungsten iso-

TABLE IV. Relative $E2$ reduced matrix element values (in barns) used in the coupled channels calculations for the ^{183}W ground state band.

I	J	Rotational model	Casten *et al.*[a]	Kerman[b]
$\frac{1}{2}^-$	$\frac{3}{2}^-$	−0.894	−0.894	−0.894
$\frac{1}{2}^-$	$\frac{5}{2}^-$	−1.095	−1.029	1.061
$\frac{3}{2}^-$	$\frac{5}{2}^-$	−0.586	0.532	−0.674
$\frac{3}{2}^-$	$\frac{7}{2}^-$	−1.434	−1.413	1.386
$\frac{5}{2}^-$	$\frac{7}{2}^-$	−0.478	−0.608	−0.629
$\frac{5}{2}^-$	$\frac{9}{2}^-$	−1.690	−1.581	1.677
$\frac{7}{2}^-$	$\frac{9}{2}^-$	−0.416	0.330	−0.617
$\frac{3}{2}^-$	$\frac{3}{2}^-$	0.894	0.874	0.897
$\frac{5}{2}^-$	$\frac{5}{2}^-$	1.171	1.145	1.176
$\frac{7}{2}^-$	$\frac{7}{2}^-$	1.380	1.349	1.385
$\frac{9}{2}^-$	$\frac{9}{2}^-$	1.557	1.522	1.563

[a]See Ref. 12.
[b]See Ref. 11.

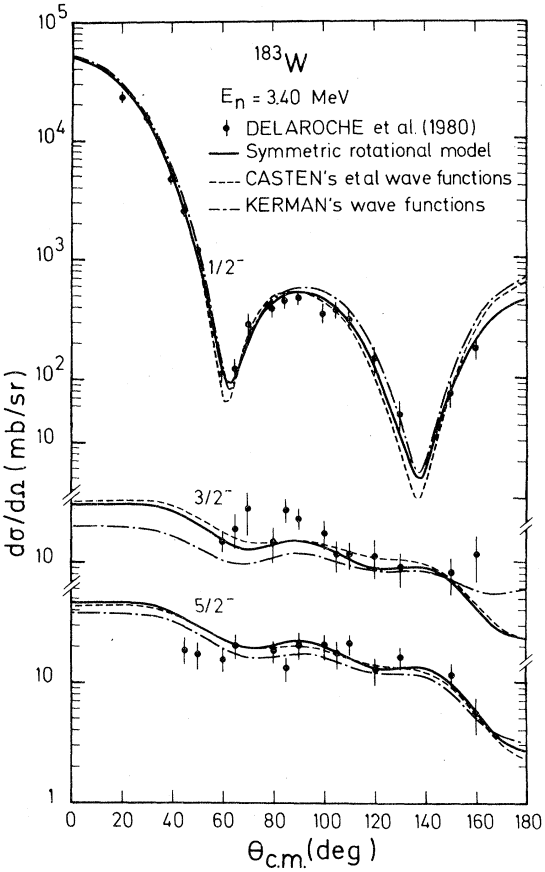

FIG. 10. Elastic scattering and inelastic scattering angular distributions from the first $\frac{3}{2}^-$ and $\frac{5}{2}^-$ states of ^{183}W at 3.4 MeV incident energy. The experimental data as well as calculations based on symmetric rotational model assumptions (full lines) are take from Ref. 1. The dashed and dotted-dashed curves result from calculations in which Casten *et al.*'s (Ref. 12) and Kerman's wave functions (Ref. 11) are used along with the $\frac{1}{2}^-$, $\frac{3}{2}^-$, $\frac{5}{2}^-$, $\frac{7}{2}^-$, and $\frac{9}{2}^-$ states of the g.s. band adopted as the coupling scheme.

topes, that the deformation parameter β_6 may be of great importance for a proper coupled channels prediction of the total cross sections σ_T at incident energies below ~700 keV. A reanalysis of the σ_T measurements of Whalen *et al.* for ^{182,184,186}W indicates that, after correction of these experimental values for self-shielding effects, a β_6 deformation is necessary to reproduce the trend of σ_T at low energies. Moreover, although small, the negative values found for β_6 have led to improved fits to the first 2^+ and 4^+ inelastic scattering cross sections at 3.4 MeV. It would be very interesting to check the present β_6 values from analyses of the (p,p') scattering measurements on ^{186}W performed at a much higher incident energy.

An important part of the present work has been devoted to the investigation of band mixing effects. From our study it appears that these effects on the total cross sections as well as inelastic scattering cross sections for the first and second excited states of the even W isotopes at 3.4 MeV are small. Concerning the odd nucleus ^{184}W, the band mixing effects on the scattering cross sections have been found to be more important. Moreover, these effects are such that no significant changes in the deformation parameters (β_2,β_4) determined in Ref. 1 are needed for improving the fits. These results confirm that the even-odd effect on β_4, found in Ref. 1, is real. This property observed on neutron scattering enhances the interest in further Hartree-Fock-Bogolyubov structure calculations involving, for ^{183}W, a blocking of the odd neutron. Finally, band mixed wave functions have also been used in CC calculations in order to estimate the direct interaction cross sections for the 0^+_β and 2^+_γ bandhead levels of the even W isotopes. In the energy range below ~4 MeV, where inelastic scattering excitation functions and angular distributions have been measured and reported, the compound nucleus mechanism dominates the neutron-nucleus interaction. For this reason it has been difficult to determine accurately the magnitude of the direct interaction cross sections. Using only the $E2$ reduced ma-

trix elements for transitions between the ground state band levels and the 0^+_β or 2^+_γ state in the CC calculations, significant contribution of the DI mechanism has been established for these excited states. Moreover, as it would be necessary to consider $E\lambda$ reduced matrix elements with $\lambda \geq 2$ for more complete analyses, it appears important to perform further CC calculations involving the coupling bases $(0^+,2^+,4^+,2^+_\gamma)$, $(0^+,2^+,4^+,0^+_\beta)$, or $(0^+,2^+,4^+,2^+_\gamma,0^+_\beta)$ in order to get proper estimates of the CN and DI cross sections for both g.s. band and vibrational states in the full energy range of interest. Such work implies a slight readjustment of the potential parameters and would require, in particular, new neutron inelastic scattering measurements for the 2^+_γ states at incident energies higher than 4 MeV where the compound nucleus mechanism is expected to vanish.

ACKNOWLEDGMENTS

The author is indebted to Dr. A. B. Smith and Dr. P. T. Guenther for helpful discussions and the provision of neutron cross sections measured for W at Argonne National Laboratory. Finally, the author thanks G. Haouat and Pr. L. Sips for a critical reading of the manuscript and suggestions, and Dr. J. Raynal for stimulating comments.

APPENDIX A

The electric multipole operators[19] $M(E\lambda)$ have been determined assuming a homogenous charge distribution[19]. These may be expressed in the laboratory system of axes as

$$M(E\lambda,\mu)=\frac{3Z}{4\pi {R_0}^3}\int_0^{R(\Omega)} r^{\lambda+2} Y^{\mu *}_\lambda(\Omega)\,dr\,d\Omega\ , \tag{A1}$$

with the following definition of the charge radius:

$$R(\Omega)=R_0\left[1+\sum_\mu \alpha^*_{2\mu} Y^\mu_2(\Omega)\right] .$$

For $\lambda=2$, a volume conservation term must be added[10,19] to (A1). An explicit formula for $\lambda=2$ and 4 can be found in Ref. 10. Expanding Eq. (A1) to the third and fourth order, respectively, and using the symbolic notations of Ref. 10, the operators $M(E6,\mu)$ and $M(E8,\mu)$ may be expressed as:

$$M(E6,\mu)=\frac{15\sqrt{35}Z{R_0}^6}{2\sqrt{286}\pi^2}\{(-)^\mu[[\alpha^{(2)}\times\alpha^{(2)}]^{(4)}\times\alpha^{(2)}]^{(6)}_{-\mu}\}$$

and

$$M(E8,\mu)=\frac{675\sqrt{5}Z{R_0}^8}{4(4862)^{1/2}\pi^{5/2}}\{(-)^\mu[[\alpha^{(2)}\times\alpha^{(2)}]^{(4)}\times[\alpha^{(2)}\times\alpha^{(2)}]^{(4)}]^{(8)}_{-\mu}\} .$$

These become, in the intrinsic collective coordinates, after lengthy but straightforward calculations,

$$\begin{aligned}M(E6,\mu)=\frac{45\sqrt{5}Z{R_0}^6}{22\sqrt{13}\pi^2}\{&D^{(6)}_{\mu 0}({\beta_0}^3+3{\beta_0}^2a'_0+3\beta_0{a'_0}^2+{a'_0}^3+\beta_0{a'_2}^2+a'_0{a'_2}^2)\\&+(\tfrac{14}{5})^{1/2}(D^{(6)}_{\mu 2}+D^{(6)}_{\mu -2})({\beta_0}^2a'_2+2\beta_0a'_2a'_0+a'_2{a'_0}^2+\tfrac{1}{6}{a'_2}^3)\\&+(\tfrac{7}{2})^{1/2}(D^{(6)}_{\mu 4}+D^{(6)}_{\mu -4})(\beta_0{a'_2}^2+a'_0{a'_2}^2)+(\tfrac{77}{18})^{1/2}(D^{(6)}_{\mu 6}+D^{(6)}_{\mu -6}){a'_2}^3\}\ ,\end{aligned}$$

and

$$M(E8,\mu)=\frac{2025ZR_0^{\,8}}{286\sqrt{17}\pi^{5/2}}\{D^{(8)}_{\mu 0}[\beta_0^{\,4}+4\beta_0^{\,3}a'_0+2\beta_0^{\,2}(3a'^{\,2}_0+a'^{\,2}_2)+4\beta_0(a'^{\,3}_0+a'_0a'^{\,2}_2)+a'^{\,4}_0+2a'^{\,2}_0a'^{\,2}_2+\tfrac{1}{6}a'^{\,4}_2]$$
$$+(\tfrac{15}{14})^{1/2}(D^{(8)}_{\mu 2}+D^{(8)}_{\mu -2})[2\beta_0^{\,3}a'_2+6\beta_0^{\,2}a'_2a'_0+\beta_0(a'^{\,3}_2+6a'_2a'^{\,2}_0)+a'_0a'^{\,3}_2+2a'_2a'^{\,3}_0]$$
$$+(\tfrac{11}{126})^{1/2}(D^{(8)}_{\mu 4}+D^{(8)}_{\mu -4})(9\beta_0^{\,2}a'^{\,2}_2+18\beta_0a'_0a'^{\,2}_2+9a'^{\,2}_0a'^{\,2}_2+a'^{\,4}_2)$$
$$+(\tfrac{143}{18})^{1/2}(D^{(8)}_{\mu 6}+D^{(8)}_{\mu -6})(\beta_0a'^{\,3}_2+a'_0a'^{\,3}_2)+(\tfrac{715}{72})^{1/2}(D^{(8)}_{\mu 8}+D^{(8)}_{\mu -8})a'^{\,4}_2\}\ .$$

The reduced matrix elements of the operators $M(E\lambda)$ defined above for $\lambda=2,4,6,8$ may be expressed as follows:

$$\langle I||M(E2)||J\rangle=A_2\hat{I}\hat{J}\beta_0\left\{C_1(I)C_1(J)\begin{bmatrix}J&2&I\\0&0&0\end{bmatrix}(1+\alpha+\alpha y^2-\alpha x^2)+C_1(I)C_2(J)\begin{bmatrix}J&2&I\\2&-2&0\end{bmatrix}x(1-2\alpha)\right.$$
$$+C_1(I)C_3(J)\begin{bmatrix}J&2&I\\0&0&0\end{bmatrix}y(1+2\alpha)+C_2(I)C_1(J)\begin{bmatrix}J&2&I\\0&2&-2\end{bmatrix}x(1-2\alpha)$$
$$+C_2(I)C_2(J)\begin{bmatrix}J&2&I\\2&0&-2\end{bmatrix}(1+\alpha+\alpha y^2-2\alpha x^2)$$
$$+C_2(I)C_3(J)\begin{bmatrix}J&2&I\\0&2&-2\end{bmatrix}(-2\alpha xy)+C_3(I)C_1(J)\begin{bmatrix}J&2&I\\0&0&0\end{bmatrix}y(1+2\alpha)$$
$$+C_3(I)C_2(J)\begin{bmatrix}J&2&I\\2&-2&0\end{bmatrix}(-2\alpha xy)$$
$$\left.+C_3(I)C_3(J)\begin{bmatrix}J&2&I\\0&0&0\end{bmatrix}(1+\alpha+3\alpha y^2-\alpha x^2)\right\},$$

$$\langle I||M(E4)||J\rangle=A_4\hat{I}\hat{J}\beta_0^{\,2}\left\{C_1(I)C_1(J)\begin{bmatrix}J&4&I\\0&0&0\end{bmatrix}(1+y^2+\tfrac{1}{6}x^2)+C_1(I)C_2(J)\begin{bmatrix}J&4&I\\2&-2&0\end{bmatrix}(\tfrac{5}{3})^{1/2}x\right.$$
$$+C_1(I)C_3(J)\begin{bmatrix}J&4&I\\0&0&0\end{bmatrix}2y+C_2(I)C_1(J)\begin{bmatrix}J&4&I\\0&2&-2\end{bmatrix}(\tfrac{5}{3})^{1/2}x$$
$$+C_2(I)C_2(J)\left[\begin{bmatrix}J&4&I\\2&0&-2\end{bmatrix}(1+y^2+\tfrac{1}{3}x^2)+(-)^J\begin{bmatrix}J&4&I\\-2&4&-2\end{bmatrix}(\tfrac{35}{18})^{1/2}x^2\right]$$
$$+C_2(I)C_3(J)\begin{bmatrix}J&4&I\\0&2&-2\end{bmatrix}(\tfrac{5}{3})^{1/2}xy+C_3(I)C_1(J)\begin{bmatrix}J&4&I\\0&0&0\end{bmatrix}2y$$
$$\left.+C_3(I)C_2(J)\begin{bmatrix}J&4&I\\2&-2&0\end{bmatrix}(\tfrac{5}{3})^{1/2}xy+C_3(I)C_3(J)\begin{bmatrix}J&4&I\\0&0&0\end{bmatrix}(1+3y^2+\tfrac{1}{6}x^2)\right\},$$

$$\langle I||M(E6)||J\rangle = A_6 \hat{I}\hat{J}\beta_0{}^3 \Bigg\{ C_1(I)C_1(J) \begin{bmatrix} J & 6 & I \\ 0 & 0 & 0 \end{bmatrix} (1+3y^2+\tfrac{1}{2}x^2)$$
$$+C_1(I)C_2(J) \begin{bmatrix} J & 6 & I \\ 2 & -2 & 0 \end{bmatrix} (\tfrac{14}{5})^{1/2}(x+xy^2+\tfrac{1}{6}x^3)$$
$$+C_1(I)C_3(J) \begin{bmatrix} J & 6 & I \\ 0 & 0 & 0 \end{bmatrix} (3y+3y^3+\tfrac{1}{2}yx^2)$$
$$+C_2(I)C_1(J) \begin{bmatrix} J & 6 & I \\ 0 & 2 & -2 \end{bmatrix} (\tfrac{14}{5})^{1/2}(x+xy^2+\tfrac{1}{6}x^3)$$
$$+C_2(I)C_2(J) \left[\begin{bmatrix} J & 6 & I \\ 2 & 0 & -2 \end{bmatrix} (1+3y^2+x^3) + (-)^J \begin{bmatrix} J & 6 & I \\ -2 & 4 & -2 \end{bmatrix} (\tfrac{7}{2})^{1/2}x^2 \right]$$
$$+C_2(I)C_3(J) \begin{bmatrix} J & 6 & I \\ 0 & 2 & -2 \end{bmatrix} (\tfrac{14}{5})^{1/2}(2xy+\tfrac{1}{6}x^3)$$
$$+C_3(I)C_1(J) \begin{bmatrix} J & 6 & I \\ 0 & 0 & 0 \end{bmatrix} (3y+3y^3+\tfrac{1}{2}yx^2)$$
$$+C_3(I)C_2(J) \begin{bmatrix} J & 6 & I \\ 2 & -2 & 0 \end{bmatrix} (\tfrac{14}{5})^{1/2}(2xy+\tfrac{1}{6}x^3)$$
$$+C_3(I)C_3(J) \begin{bmatrix} J & 6 & I \\ 0 & 0 & 0 \end{bmatrix} (1+9y^2+\tfrac{1}{2}x^2) \Bigg\},$$

$$\langle I||M(E8)||J\rangle = A_8 \hat{I}\hat{J}\beta_0{}^4 \Bigg\{ C_1(I)C_1(J) \begin{bmatrix} J & 8 & I \\ 0 & 0 & 0 \end{bmatrix} (1+6y^2+x^2+x^2y^2+3y^4+\tfrac{1}{12}x^4)$$
$$+C_1(I)C_2(J) \begin{bmatrix} J & 8 & I \\ 2 & -2 & 0 \end{bmatrix} (\tfrac{30}{7})^{1/2}(x+\tfrac{1}{2}x^3+3xy^2)$$
$$+C_1(I)C_3(J) \begin{bmatrix} J & 8 & I \\ 0 & 0 & 0 \end{bmatrix} (4y+12y^3+2yx^2)$$
$$+C_2(I)C_1(J) \begin{bmatrix} J & 8 & I \\ 0 & 2 & -2 \end{bmatrix} (\tfrac{30}{7})^{1/2}(x+\tfrac{1}{2}x^3+3xy^2)$$
$$+C_2(I)C_2(J) \Bigg[\begin{bmatrix} J & 8 & I \\ 2 & 0 & -2 \end{bmatrix} (1+6y^2+2x^2+3y^4+2x^2y^2+\tfrac{1}{4}x^4)$$
$$+(-)^J \begin{bmatrix} J & 8 & I \\ -2 & 4 & -2 \end{bmatrix} (x^2+x^2y^2+\tfrac{1}{6}x^4)(\tfrac{99}{14})^{1/2} \Bigg]$$
$$+C_2(I)C_3(J) \begin{bmatrix} J & 8 & I \\ 0 & 2 & -2 \end{bmatrix} (\tfrac{30}{7})^{1/2}(3xy+\tfrac{1}{2}yx^3+3xy^3)$$
$$+C_3(I)C_1(J) \begin{bmatrix} J & 8 & I \\ 0 & 0 & 0 \end{bmatrix} (4y+12y^3+2yx^2)$$
$$+C_3(I)C_2(J) \begin{bmatrix} J & 8 & I \\ 2 & -2 & 0 \end{bmatrix} (\tfrac{30}{7})^{1/2}(3xy+\tfrac{1}{2}yx^3+3xy^3)$$
$$+C_3(I)C_3(J) \begin{bmatrix} J & 8 & I \\ 0 & 0 & 0 \end{bmatrix} (1+18y^2+x^2+15y^4+3x^2y^2+\tfrac{1}{12}x^4) \Bigg\}$$

The definition of the following symbols: $C_i(I)$, α, x, y, and β_0 can be found in Ref. 10. With an exception for the band-mixing amplitudes $C_i(I)$ which are computed numerically (see Ref. 10), these parameters are fitted on some experimental measurements. In the expressions given above, the coefficients A_2, A_4, A_6, and A_8 are defined as

$$A_2=\frac{3ZR_0^2}{4\pi},\quad A_4=\frac{27ZR_0^4}{28\pi^{3/2}},\quad A_6=\frac{45\sqrt{5}ZR_0^6}{22\sqrt{13}\pi^2},\quad A_8=\frac{2025ZR_0^8}{286\sqrt{17}\pi^{5/2}},$$

and the quantity

$$\begin{bmatrix} j_1 & j_2 & j_3 \\ m_1 & m_2 & m_3 \end{bmatrix}$$

represents the usual "3j" symbol. Finally, the symbol $\hat{I}$ used above is defined as $\hat{I}=(2I+1)^{1/2}$.

APPENDIX B

A straightforward method for derivating the ^{183}W reduced matrix elements of the electric quadrupole operator[19] $M(E2)$ in a form suitable for the ECIS 78 calculations is explained. This is achieved by combining the general (and usual) definition[21] of the reduced transition probability $B(E2)$:

$$B(E2;I\rightarrow J)=\frac{1}{(2I+1)}\,|\,\langle J||M(E2)||I\rangle\,|^2\,, \tag{B1}$$

with a more specific relation suitable for transitions occurring in odd mass deformed nuclei.[23] Given in e^2b^2 units, $B(E2)$ can be expressed for band-mixed states (ν,I) and (ν',J) as follows:

$$\begin{aligned} B(E2;\nu,I\rightarrow\nu',J)=\frac{5}{16\pi}\,|\sum_{KK'} & C_{\nu'}(0,K';J)C_{\nu}(0,K;I)Q^{K'K} \\ & \times[\,(IK2,K'-K\,|\,JK')+(-)^{J+K'}(IK2,-K'-K\,|\,J,-K')b_{E2} \\ & \times(\delta_{K,1/2}\delta_{K',3/2}+\delta_{K,3/2}\delta_{K',1/2})]\,|^2\,. \end{aligned} \tag{B2}$$

The symbols entering Eq. (B2) have been defined in Ref. 23. The mixing amplitudes C_ν values involved presently have been derived[11,12] from fitting the energy of the ^{183}W states. The $Q^{K'K}$ and b_{E2} values used have been determined experimentally by McGowan *et al.*[3] The labels ν and (ν') refer to the high (H) and low (L) energy states of the same spin and parity. As only the ground state band transitions have just been considered in the present work, it follows that

$$\nu=\nu'=L\,.$$

From Eqs. (B1) and (B2) one may obtain the off-diagonal matrix elements of the $M(E2)$ operator. These have been defined as follows:

$$\begin{aligned} \langle J||M(E2)||I\rangle=\left[\frac{5}{16\pi}(2I+1)\right]^{1/2}\Bigg\{ & \sum_{KK'} C_L(0,K',J)C_L(0,K,I)Q^{K'K} \\ & \times[\,(IK2,K'-K\,|\,JK')+(-)^{J+K'}(IK2,-K'-K\,|\,J,-K')b_{E2} \\ & \times(\delta_{K,1/2}\delta_{k',3/2}+\delta_{K,3/2}\delta_{K',1/2})]\Bigg\}\,, \end{aligned} \tag{B3}$$

in which the index $K(K')$ runs over the values $\frac{1}{2}$ and $\frac{3}{2}$. The reorientation matrix elements $\langle I||M(E2)||I\rangle$

have to be determined from the Q^{KK} values obtained by McGowan *et al.*[3] in the rotational model framework. If $Q^{1/2\,1/2}$ is noted as $\langle Q_0 \rangle$, the average values of the intrinsic quadrupole moments for ^{182}W and ^{184}W, the spectroscopic quadrupole moments Q_I can be expressed as:

$$Q_I = \langle Q_0 \rangle \left[\frac{3K^2 - I(I+1)}{(I+1)(2I+3)} \right] , \tag{B4}$$

under the rotational model assumption.

From the identification of (B4) to the model independent relationship[21]

$$Q_I = \left[\frac{16\pi}{5} \right]^{1/2} \left[\frac{I(2I-1)}{(I+1)(2I+1)(2I+3)} \right]^{1/2} \langle I||M(E2)||I \rangle ,$$

it turns out that

$$\langle I||M(E2)||I \rangle = \left[\frac{5}{16\pi} \right]^{1/2} \langle Q_0 \rangle [3K^2 - I(I+1)] \left[\frac{(2I+1)}{I(2I-1)(I+1)(2I+3)} \right]^{1/2} .$$

[1] J. P. Delaroche, G. Haouat, J. Lachkar, Y. Patin, J. Sigaud, and J. Chardine, Phys. Rev. C 23, 136 (1981).

[2] K. Kumar and M. Baranger, Nucl. Phys. A122, 273 (1968).

[3] F. K. McGowan, C. E. Bemis, Jr., J. L. C. Ford, Jr, W. T. Milner, D. Shapira, and P. H. Stelson, Phys. Rev. C 20, 2093 (1979), and references cited therein.

[4] S. F. Mughabghab and D. I. Garber, Brookhaven National Laboratory Report No. BNL-325, 1973, 3rd ed., Vol. 1.

[5] J. Whalen and J. Meadows, Argonne National Laboratory Report No. ANL-7210, 1966.

[6] W. Glasgow and D. Graham Foster, Phys. Rev. C 3, 604 (1971).

[7] R. C. Martin, Ph. D. thesis, Rensselaer Polytechnic Institute, 1967 (unpublished); Bull. Am. Phys. Soc. 12, 106 (1967).

[8] P. A. Guenther and A. B. Smith, Bull. Am. Phys. Soc. 23, 944 (1978).

[9] K. Kumar, Phys. Lett. 29B, 25 (1969).

[10] A. Faessler, W. Greiner, and R. K. Sheline, Nucl. Phys. 70, 33 (1965).

[11] A. K. Kerman, K. Dan. Vidensk. Selsk. Mat. Fys. Medd. 30, No. 15 (1956).

[12] R. F. Casten, P. Kleinheinz, P. J. Daly, and B. Elbek, K. Dan. Vidensk. Selsk. Mat. Fys. Medd. 38, No. 13 (1972).

[13] J. Raynal, ECIS 78 (unpublished).

[14] F. T. Baker, T. H. Kruse, W. Harting, I. Y. Lee, and J. X. Saladin, Nucl. Phys. A258, 43 (1976).

[15] F. T. Baker, Nucl. Phys. A331, 39 (1979), and references cited therein.

[16] D. L. Hillis, E. E. Gross, D. C. Hensley, C. R. Bingham, F. T. Baker, and A. Scott, Phys. Rev. C 16, 1467 (1977).

[17] P. T. Deason, Jr., Ph. D. thesis, Michigan State University, 1979 (unpublished).

[18] M. C. Mirzaa, J. P. Delaroche, S. W. Yates, J. L. Weil, and M. T. McEllistrem, Bull. Am. Phys. Soc. 25, 542 (1980); M. T. McEllistrem, J. P. Delaroche, M. C. Mirzaa, and S. W. Yates, in Proceedings of the International Conference on Nuclear Physics, Abstracts, Berkeley, 1980, LBL Report No. LBL-11118, 1980, Vol. I, p. 886.

[19] J. M. Heisenberg and W. Greiner, *Nuclear Models* (North-Holland, Amsterdam, 1970), p. 56.

[20] A. Winther and J. De Boer, *Coulomb Excitations,* edited by K. Alder and A. Winther (Academic, New York, 1966), p. 305.

[21] K. Kumar, in the *Electromagnetic Interaction in Nuclear Spectroscopy,* edited by W. D. Hamilton (North-Holland, Amsterdam, 1975), p. 55.

[22] M. Sakai and A. C. Rester, At. Data Nucl. Data Tables 20, 441 (1977).

[23] R. T. Brockmeier, S. Wahlborn, E. J. Seppi, and F. Boehm, Nucl. Phys. 63, 102 (1965).

[24] D. J. Rowe, Nucl. Phys. 61, 1 (1965).

[25] T. Tamura, Rev. Mod. Phys. 37, 679 (1965).

[26] J. J. O'Brien, J. X. Saladin, C. Baktash, and J. G. Alessi, Phys. Rev. Lett. 38, 324 (1977).

[27] W. T. Milner, F. K. McGowan, R. L. Robinson, P. H. Stelson, and R. O. Sayer, Nucl. Phys. A177, 1 (1971).

[28] F. K. McGowan, W. T. Milner, R. O. Sayer, R. L. Robinson, and P. H. Stelson, Bull. Am. Phys. Soc. 14, 1204 (1969).

[29] P. H. Stelson and L. Grodzins, Nucl. Data A1, 21 (1965).

[30] L. W. Oberley, N. H. Hershkowitz, S. A. Wender, and A. B. Carpenter, Phys. Rev. C 3, 1585 (1971).

[31] P. T. Guenther, A. B. Smith, and J. F. Whalen, Argonne National Laboratory Report No. ANL/NDM-56, 1981.

[32]L. Dresner, Nucl. Instrum. Methods 16, 176 (1962); R. L. Macklin, *ibid.* 26, 213 (1964).

[33]D. L. Hendrie, B. G. Harvey, J. C. Faivre, and J. Mahoney, UCRL Report No. UCRL-20426, 1970, p. 87.

[34]R. M. Ronningen, G. M. Crowley, J. E. Finck, C. H. King, R. C. Melin, J. A. Nolen, Jr., P. T. Deason, and F. M. Bernthal, Bull. Am. Phys. Soc. 24, 668 (1979).

[35]S. G. Nilsson, C. F. Tsang, A. Sobiczewski, S. Wycech, C. Gustafson, I. L. Lamm, P. Möller, Z. Szymanski, and B. Nilsson, Nucl. Phys. A131, 1 (1969).

[36]P. T. Guenther, Ph. D. thesis, University of Illinois, Chicago, 1977 (unpublished).

[37]D. Lister, A. Smith, and C. Dunford, Phys. Rev. 162, 1077 (1967).

[38]W. Hauser and H. Feshbach, Phys. Rev. 87, 366 (1952).

[39]P. L. Ottaviani and L. Zuffi, Nucl. Phys. A152, 570 (1970).

[40]R. F. Casten and D. D. Warner, Nucl. Phys. A333, 237 (1980).